

Decay of the monochromatic capillary wave

A. I. Dyachenko⁺, A. O. Korotkevich⁺¹⁾, V. E. Zakharov⁺*

⁺*L.D. Landau Institute for Theoretical Physics RAS, 119334 Moscow, Russia*

^{*}*University of Arizona, Department of Mathematics, Tucson, USA*

Submitted 31 March 2003

It was demonstrated by the direct numerical simulation that in the case of weakly nonlinear capillary waves one can get resonant waves interaction on the discrete grid when resonant conditions never fulfilled exactly. The waves decay pattern was obtained. The influence of the mismatch of resonant condition was studied as well.

PACS: 47.20.-k, 47.35.+i

The nonlinear waves on the surface of fluid are one of the most well known and complex phenomena in nature. Mature ocean waves and ripples on the surface of the tea in the pot, for example, can be described by very similar equations. Both these phenomena are substantially nonlinear, but the wave amplitude usually significantly less than the wave length. At this condition waves are weakly nonlinear.

To describe the processes of this kind the weak turbulence theory was proposed [1, 2]. It results to Kolmogorov spectra as an exact solution of the Hasselman-Zakharov kinetic equation [3]. Many experimental result are in great accordance with this theory. In the case of gravity surface waves the first confirmation was obtained by Toba [4], the most recent data by Hwang [5] have been received as a result of lidar scanning of ocean surface. Recent experiments with capillary waves on the surface of liquid hydrogen [6, 7] are also in good agreement with this theory. From the other hand some numerical calculations have been made to check the validity of the weak turbulent theory [8–10].

In this Letter we study the one of the keystones of the weak turbulent theory, the resonant interaction of weakly nonlinear waves. The question under study is the following:

- How discrete grid for wavenumbers in numerical simulations affects the resonant interaction?
- Can nonlinear frequency shift broad resonant manifold to make discreteness unimportant?

We study this problem for nonlinear capillary waves on the surface of the infinitely depth incompressible ideal fluid. Direct numerical simulation can make the situation clear.

Let us consider the irrotational flow of an ideal incompressible fluid of infinite depth. For the sake of simplicity let us suppose fluid density $\rho = 1$. The velocity potential ϕ satisfies Laplas equation

$$\Delta\phi = 0 \quad (1)$$

in the fluid region, bounded by

$$-\infty < z < \eta(\mathbf{r}), \quad \mathbf{r} = (x, y), \quad (2)$$

with the boundary conditions for the velocity potential

$$\begin{aligned} \frac{\partial\eta}{\partial t} + \frac{\partial\phi}{\partial x} \frac{\partial\eta}{\partial x} + \frac{\partial\phi}{\partial y} \frac{\partial\eta}{\partial y} &= \frac{\partial\phi}{\partial z} \Big|_{z=\eta}, \\ \left(\frac{\partial\phi}{\partial t} + \frac{1}{2}(\nabla\phi)^2 \right) \Big|_{z=\eta} &+ \\ + \sigma(\sqrt{1 + (\nabla\eta)^2} - 1) &= 0, \end{aligned} \quad (3)$$

on $z = \eta$, and

$$\phi_z|_{z=-\infty} = 0, \quad (4)$$

on $z \rightarrow -\infty$. Here $\eta = \eta(x, y, t)$ is the surface displacement. In the case of capillary waves the Hamiltonian has the form

$$H = T + U,$$

$$T = \frac{1}{2} \int d^2r \int_{-\infty}^{\eta} (\nabla\phi)^2 dz, \quad (5)$$

$$U = \sigma \int (\sqrt{1 + (\nabla\eta)^2} - 1) d^2r, \quad (6)$$

where σ – is the surface tension coefficient. In [11], it was shown that this system is Hamiltonian one. The Hamiltonian variables are the displacement of the surface $\eta(x, y, t)$ and velocity potential on the surface of

¹⁾e-mail: kao@landau.ac.ru

the fluid $\psi(x, y; t) = \phi(x, y, \eta(x, y; t); t)$. Hamiltonian equations are the following

$$\frac{\partial \eta}{\partial t} = \frac{\delta H}{\delta \psi}, \quad \frac{\partial \psi}{\partial t} = -\frac{\delta H}{\delta \eta}. \quad (7)$$

Using the weak nonlinearity assumption [3] one can expand the Hamiltonian in the powers of surface displacement

$$H = \frac{1}{2} \int (\sigma |\nabla \eta|^2 + \psi \hat{k} \psi) d^2 r + \frac{1}{2} \int \eta [|\nabla \psi|^2 - (\hat{k} \psi)^2] d^2 r. \quad (8)$$

The third order is enough for three-wave interactions. Here \hat{k} is the linear operator corresponding to multiplying of Fourier harmonics by modulus of the wavenumber \mathbf{k} . Using (7) one can get the following system of dynamical equations

$$\begin{aligned} \dot{\eta} &= \hat{k} \psi - \operatorname{div}(\eta \nabla \psi) - \hat{k}[\eta \hat{k} \psi], \\ \dot{\psi} &= \sigma \Delta \eta - \frac{1}{2} [(\nabla \psi)^2 - (\hat{k} \psi)^2] \end{aligned} \quad (9)$$

The properties of \hat{k} -operator suggest to exploit the equations in Fourier space for Fourier components of η and ψ

$$\psi_{\mathbf{k}} = \frac{1}{2\pi} \int \psi_{\mathbf{r}} e^{i\mathbf{k}\mathbf{r}} d^2 r, \quad \eta_{\mathbf{k}} = \frac{1}{2\pi} \int \eta_{\mathbf{r}} e^{i\mathbf{k}\mathbf{r}} d^2 r.$$

Let us introduce the canonical variables $a_{\mathbf{k}}$ as shown below

$$a_{\mathbf{k}} = \sqrt{\frac{\omega_k}{2k}} \eta_{\mathbf{k}} + i \sqrt{\frac{k}{2\omega_k}} \psi_{\mathbf{k}}, \quad (10)$$

where

$$\omega_k = \sqrt{\sigma k^3}. \quad (11)$$

With these variables the Hamiltonian (8) acquires the following form

$$\begin{aligned} H &= \int \omega_k |a_{\mathbf{k}}|^2 d\mathbf{k} + \\ &+ \frac{1}{6} \frac{1}{2\pi} \int E_{\mathbf{k}_1 \mathbf{k}_2}^{k_0} (a_{\mathbf{k}_1} a_{\mathbf{k}_2} a_{\mathbf{k}_0} + a_{\mathbf{k}_1}^* a_{\mathbf{k}_2}^* a_{\mathbf{k}_0}^*) \times \\ &\quad \times \delta(\mathbf{k}_1 + \mathbf{k}_2 + \mathbf{k}_0) d\mathbf{k}_1 d\mathbf{k}_2 d\mathbf{k}_0 + \\ &+ \frac{1}{2} \frac{1}{2\pi} \int M_{\mathbf{k}_1 \mathbf{k}_2}^{k_0} (a_{\mathbf{k}_1} a_{\mathbf{k}_2} a_{\mathbf{k}_0}^* + a_{\mathbf{k}_1}^* a_{\mathbf{k}_2}^* a_{\mathbf{k}_0}) \times \\ &\quad \times \delta(\mathbf{k}_1 + \mathbf{k}_2 - \mathbf{k}_0) d\mathbf{k}_1 d\mathbf{k}_2 d\mathbf{k}_0. \end{aligned} \quad (12)$$

Here

$$\begin{aligned} E_{\mathbf{k}_1 \mathbf{k}_2}^{k_0} &= V_{\mathbf{k}_1 \mathbf{k}_2}^{k_0} + V_{\mathbf{k}_0 \mathbf{k}_2}^{k_1} + V_{\mathbf{k}_0 \mathbf{k}_1}^{k_2}, \\ M_{\mathbf{k}_1 \mathbf{k}_2}^{k_0} &= V_{\mathbf{k}_1 \mathbf{k}_2}^{k_0} - V_{-\mathbf{k}_0 \mathbf{k}_2}^{k_1} - V_{-\mathbf{k}_0 \mathbf{k}_1}^{k_2}, \\ V_{\mathbf{k}_1 \mathbf{k}_2}^{k_0} &= \sqrt{\frac{\omega_{k_1} \omega_{k_2} k_0}{8k_1 k_2 \omega_{k_0}}} L_{\mathbf{k}_1 \mathbf{k}_2}, \\ L_{\mathbf{k}_1 \mathbf{k}_2} &= (\mathbf{k}_1 \mathbf{k}_2) + |\mathbf{k}_1| |\mathbf{k}_2|. \end{aligned} \quad (13)$$

The dynamic equations in this variables can be easily obtained by variation of Hamiltonian

$$\begin{aligned} \dot{a}_{\mathbf{k}} &= -i \frac{\delta H}{\delta a_{\mathbf{k}}^*} = -i \omega_k a_{\mathbf{k}} - \\ &- \frac{i}{2} \frac{1}{2\pi} \int M_{\mathbf{k}_1 \mathbf{k}_2}^{\mathbf{k}} a_{\mathbf{k}_1} a_{\mathbf{k}_2} \delta(\mathbf{k}_1 + \mathbf{k}_2 - \mathbf{k}) d\mathbf{k}_1 d\mathbf{k}_2 - \\ &- \frac{i}{2\pi} \int M_{\mathbf{k} \mathbf{k}_2}^{k_0} a_{\mathbf{k}_2}^* a_{\mathbf{k}_0} \delta(\mathbf{k} + \mathbf{k}_2 - \mathbf{k}_0) d\mathbf{k}_2 d\mathbf{k}_0 - \\ &- \frac{i}{2} \frac{1}{2\pi} \int E_{\mathbf{k}_1 \mathbf{k}_2}^{\mathbf{k}} a_{\mathbf{k}_1}^* a_{\mathbf{k}_2}^* \delta(\mathbf{k}_1 + \mathbf{k}_2 + \mathbf{k}) d\mathbf{k}_1 d\mathbf{k}_2. \end{aligned} \quad (14)$$

Each term in this equation has their own clear physical meaning. Linear term gives a periodic evolution of the initial wave. The first nonlinear term describes a merging of two waves \mathbf{k}_1 and \mathbf{k}_2 in \mathbf{k} . The second-decay of the wave \mathbf{k}_0 to the waves \mathbf{k} and \mathbf{k}_2 . And the last term corresponds to the second harmonic generation process. It is useful to eliminate the linear term by the following substitution

$$a_{\mathbf{k}} = A_{\mathbf{k}} e^{i\omega_k t}. \quad (15)$$

In this variables the dynamical equations take the form

$$\begin{aligned} \dot{A}_{\mathbf{k}} &= -\frac{i}{2} \frac{1}{2\pi} \int M_{\mathbf{k}_1 \mathbf{k}_2}^{\mathbf{k}} A_{\mathbf{k}_1} A_{\mathbf{k}_2} e^{i\Omega_{\mathbf{k}_1 \mathbf{k}_2}^{\mathbf{k}} t} \times \\ &\quad \times \delta(\mathbf{k}_1 + \mathbf{k}_2 - \mathbf{k}) d\mathbf{k}_1 d\mathbf{k}_2 - \\ &- \frac{i}{2\pi} \int M_{\mathbf{k} \mathbf{k}_2}^{k_0} A_{\mathbf{k}_2}^* A_{\mathbf{k}_0} e^{-i\Omega_{\mathbf{k} \mathbf{k}_2}^{k_0} t} \times \\ &\quad \times \delta(\mathbf{k} + \mathbf{k}_2 - \mathbf{k}_0) d\mathbf{k}_2 d\mathbf{k}_0, \end{aligned} \quad (16)$$

where

$$\Omega_{\mathbf{k}_1 \mathbf{k}_2}^{k_0} = \omega_{k_1} + \omega_{k_2} - \omega_{k_0}. \quad (17)$$

Here we do not consider the harmonic generation term. The remaining terms give us the following conditions of resonance

$$\Omega_{\mathbf{k}_1 \mathbf{k}_2}^{\mathbf{k}} = \omega_{k_1} + \omega_{k_2} - \omega_k = 0, \quad \mathbf{k}_1 + \mathbf{k}_2 - \mathbf{k} = 0. \quad (18)$$

All this theory is well known in the literature [3].

Now let us turn to the discrete grid. Also, from this point we assume periodic boundary conditions in x and

y with lengths L_x and L_y . One can easily obtain the equations similar to (16)

$$\begin{aligned} \dot{A}_{\mathbf{k}} = & -\frac{i}{2} \frac{2\pi}{L_x L_y} \sum_{\mathbf{k}_1 \mathbf{k}_2} M_{\mathbf{k}_1 \mathbf{k}_2}^{\mathbf{k}} A_{\mathbf{k}_1} A_{\mathbf{k}_2} e^{i\Omega_{\mathbf{k}_1 \mathbf{k}_2}^{\mathbf{k}} t} \times \\ & \times \Delta_{(\mathbf{k}_1 + \mathbf{k}_2), -\mathbf{k}} - \\ & - \frac{i2\pi}{L_x L_y} \sum_{\mathbf{k}_2 \mathbf{k}_0} M_{\mathbf{k}_2 \mathbf{k}_0}^{\mathbf{k}} A_{\mathbf{k}_2}^* A_{\mathbf{k}_0} e^{-i\Omega_{\mathbf{k}_2 \mathbf{k}_0}^{\mathbf{k}} t} \Delta_{(\mathbf{k} + \mathbf{k}_2), -\mathbf{k}_0}, \end{aligned} \quad (19)$$

where $\Delta_{\mathbf{k}_1, \mathbf{k}_2}$ is the Kronecker delta – the discrete analogue of Dirac delta function.

Consider the decay of a monochromatic capillary wave $A_{\mathbf{k}_0}$ on two waves

$$\begin{aligned} \dot{A}_{\mathbf{k}_0} &= -\frac{i}{2} \frac{2\pi}{L_x L_y} M_{\mathbf{k}_1 \mathbf{k}_2}^{\mathbf{k}_0} A_{\mathbf{k}_1} A_{\mathbf{k}_2} e^{i\Omega_{\mathbf{k}_1 \mathbf{k}_2}^{\mathbf{k}_0} t}, \\ \dot{A}_{\mathbf{k}_1} &= -i \frac{2\pi}{L_x L_y} M_{\mathbf{k}_1 \mathbf{k}_2}^{\mathbf{k}_0} A_{\mathbf{k}_2}^* A_{\mathbf{k}_0} e^{-i\Omega_{\mathbf{k}_1 \mathbf{k}_2}^{\mathbf{k}_0} t}, \\ \dot{A}_{\mathbf{k}_2} &= -i \frac{2\pi}{L_x L_y} M_{\mathbf{k}_1 \mathbf{k}_2}^{\mathbf{k}_0} A_{\mathbf{k}_1}^* A_{\mathbf{k}_0} e^{-i\Omega_{\mathbf{k}_1 \mathbf{k}_2}^{\mathbf{k}_0} t}. \end{aligned} \quad (20)$$

Let $A_{\mathbf{k}_1}, A_{\mathbf{k}_2}$ be small ($|A_{\mathbf{k}_0}| \gg \max(|A_{\mathbf{k}_1}|, |A_{\mathbf{k}_2}|)$ at $t = 0$). In this case the equations can be linearized. The solution of linearized (20) has the following form ($A_{\mathbf{k}_0} \sim \text{const}$)

$$A_{\mathbf{k}_{1,2}}(t) = A_{\mathbf{k}_{1,2}}(0) e^{\lambda t}, \quad (21)$$

where

$$\begin{aligned} \lambda = & -\frac{i}{2} \Omega_{\mathbf{k}_1 \mathbf{k}_2}^{\mathbf{k}_0} + \\ & + \sqrt{\left| \frac{2\pi}{L_x L_y} M_{\mathbf{k}_1 \mathbf{k}_2}^{\mathbf{k}_0} A_{\mathbf{k}_0} \right|^2 - \left(\frac{1}{2} \Omega_{\mathbf{k}_1 \mathbf{k}_2}^{\mathbf{k}_0} \right)^2}. \end{aligned} \quad (22)$$

In the case of a continuous media resonant conditions (18) can be satisfied exactly. But on the grid there is always frequency mismatch $\Omega_{\mathbf{k}_1 \mathbf{k}_2}^{\mathbf{k}_0} \neq 0$. Though if the amplitude of initial wave is high enough there are resonances even on a discrete grid. But the width of this resonance is very important.

System of equations (9) can be solved numerically. This system is nonlocal in coordinate space due to the presence of the \hat{k} -operator. The origin of this operator gives us a hint to solve (9) in wavenumbers space (K -space). In this case we can effectively use fast Fourier transform algorithm. Omitting the details of this numerical scheme, we reproduce only the final results of calculations.

We have solved system of equations (9) numerically in the dimensionless periodic domain $2\pi \times 2\pi$ (the wavenumbers k_x and k_y are integer numbers in this case). Correspondantly, all other variables also become dimensionless. It is convenient to use surfacetension $\sigma = 1$.

The size of the grid was chosen 512×512 points. We have also included damping for waves with large wave numbers. In K -space damping terms for $\eta_{\mathbf{k}}$ and $\psi_{\mathbf{k}}$ respectively were the following: $\gamma_{\mathbf{k}} \eta_{\mathbf{k}}$ and $\gamma_{\mathbf{k}} \psi_{\mathbf{k}}$. Where $\gamma_{\mathbf{k}}$ was of the following form

$$\begin{aligned} \gamma_{\mathbf{k}} &= 0, |\mathbf{k}| < \frac{1}{2} |\mathbf{k}_{\max}|, \\ \gamma_{\mathbf{k}} &= -\gamma_0 (|\mathbf{k}| - \frac{1}{2} |\mathbf{k}_{\max}|)^2, |\mathbf{k}| \geq \frac{1}{2} |\mathbf{k}_{\max}|, \end{aligned} \quad (23)$$

where γ_0 is some constant.

As an initial conditions we used one monochromatic wave of sufficiently large amplitude with wave-numbers \mathbf{k}_0 ($k_{0x} = 0, k_{0y} = 68$). Along with that there was a small random noise in all other harmonics.

Resonant manifold (18) for decaying waves

$$\begin{aligned} \mathbf{k}_0 &= \begin{pmatrix} 0 \\ k_0 \end{pmatrix}, \\ \mathbf{k}_1 &= \begin{pmatrix} -k_x \\ k_0 - k_y \end{pmatrix}, \mathbf{k}_2 = \begin{pmatrix} k_x \\ k_0 + k_y \end{pmatrix} \end{aligned} \quad (24)$$

is given at Fig.1. Since the wave numbers are integers, the resonant curve never coincides with grid points ex-

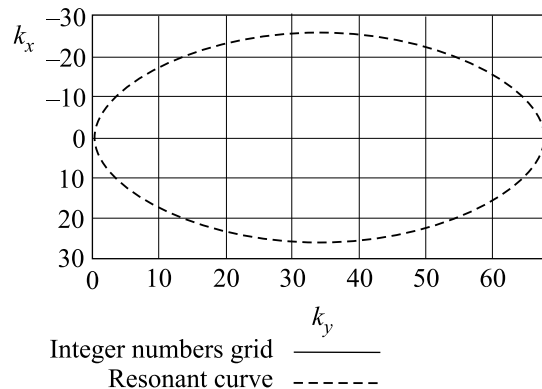


Fig.1. The resonant manifold for $k_0 = 68$

actly. The detail picture is given on Fig.2. It is clear, that some points are closer to the resonant manifold than the other. It is the difference might be important in numerics.

In the beginning one can observe exponential growth of resonant harmonics in accordance with (21) and (22). This is shown in Fig.3 and Fig.4. Here one can clearly see some harmonics are in resonance and others are not.

Than almost all harmonics in the resonant manifold become involved in decay process Fig.5. Later on the harmonics which are the closest to the resonant manifold (compare with Fig.2) reach the maximum level while the

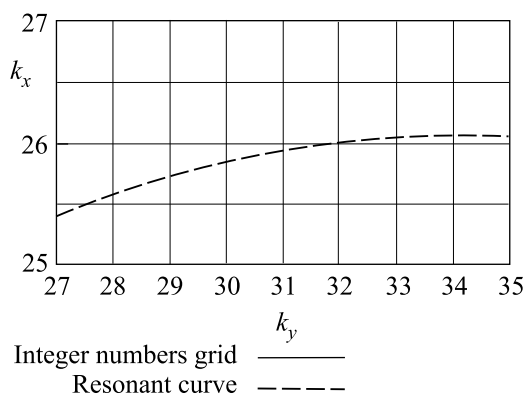
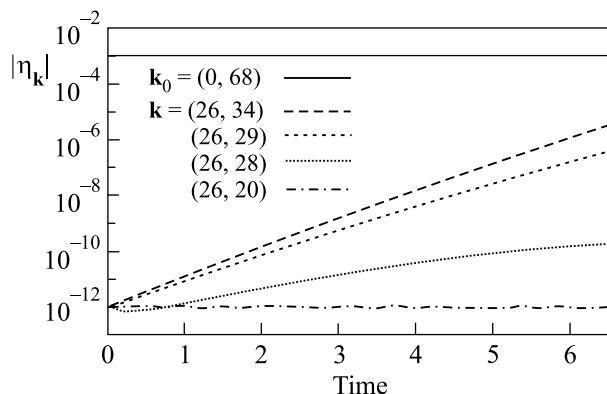
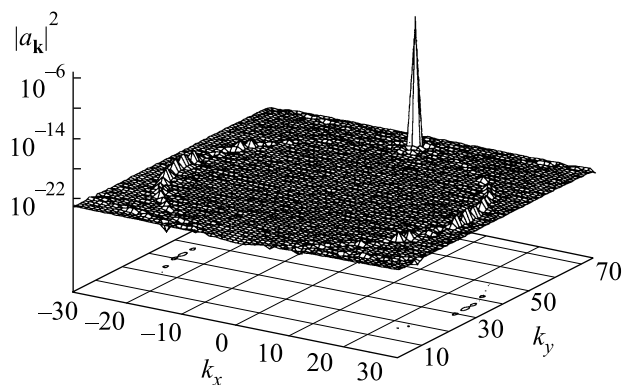
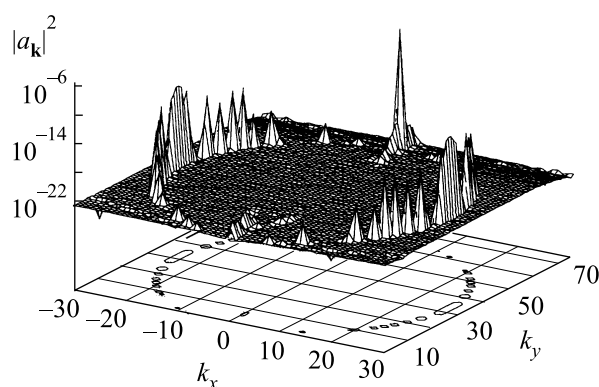
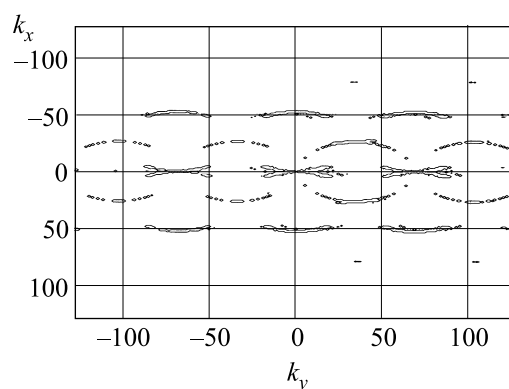


Fig.2. Different mismatch is seen at different grid points

Fig.3. Evolution of various harmonics for decaying wave $\mathbf{k}_0 = (0, 68)$

secondary decay process develops. Waves amplitudes became significantly different. The largest amplitudes are for those waves with the maximal growth rate. One can see regular structure generated by that \mathbf{k}_0 wave in Fig.6. After a while the whole k -space is filled by decaying waves, as shown in Fig.7.

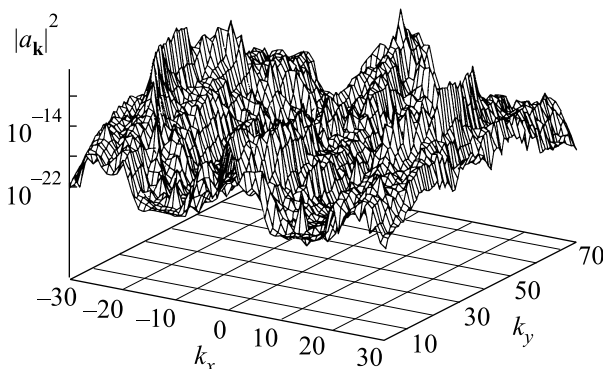
Direct numerical simulation has demonstrated that finite width of the resonance makes discrete grid very

Fig.4. Resonant harmonics starting to grow. At the basement there is contour line for level $|a_k|^2 = 10^{-22}$. Time $t = 1.4$ Fig.5. Secondary decays start. At the basement there is contour line for level $|a_k|^2 = 10^{-22}$. Time $t = 11$ Fig.6. The contour lines for $|a_k|^2 = 10^{-21}$. Secondary decays are clearly seen. Time $t = 14$

similar to continuous. Of course, it is true only if the amplitude of the wave is large enough, so that according to (22)

$$\left| \frac{2\pi}{L_x L_y} M_{\mathbf{k}_1 \mathbf{k}_2}^{\mathbf{k}_0} A_{\mathbf{k}_0} \right| > \left| \frac{1}{2} \Omega_{\mathbf{k}_1 \mathbf{k}_2}^{\mathbf{k}_0} \right|. \quad (25)$$

As regards numerical simulation of the turbulence, namely weak turbulence; the condition (25) is very important. $A_{\mathbf{k}_0}$ has to be treated as level of turbulence.

Fig.7. Wave numbers spectrum at time $t = 57$

Authors want to thank Prof. E. A. Kuznetsov for very helpful discussions. This work was supported by RFBR grant # 03-01-00289, INTAS grant # 00-292, the Programme “Nonlinear dynamics and solitons” from the RAS Presidium and “Leading Scientific Schools of Russia” grant, also by US Army Corps of Engineers, RDT&E Programm, Grant DACA # 42-00-C0044 and by NSF Grant # NDMS0072803.

-
1. V. E. Zakharov and N. N. Filonenko, Dokl. Akad. Nauk SSSR **170**, 1292 (1966).
 2. V. E. Zakharov and N. N. Filonenko, J. Appl. Mech. Tech. Phys. **4**, 506 (1967).
 3. V. E. Zakharov, G. Falkovich, and V. S. Lvov, *Kolmogorov Spectra of Turbulence I*, Springer-Verlag, Berlin, 1992.
 4. Y. Toba, J. Oceanogr. Soc. Jpn. **29**, 209 (1973).
 5. P. A. Hwang, D. W. Wang, E. J. Walsh et al., J. Phys. Oceanogr. **30**, 2753 (2000).
 6. M. Yu. Brazhnikov, G. V. Kolmakov, A. A. Levchenko, and L. P. Mezhev-Deglin, Pis'ma v ZhETF **74**, 12, 660 (2001); (english transl. JETP Lett. **74**, 12, 583 (2001)).
 7. M. Yu. Brazhnikov, G. V. Kolmakov, and A. A. Levchenko, ZhETF **122**, 521 (2002); (english transl. JETP **95**, 447 (2002)).
 8. A. N. Pushkarev and V. E. Zakharov, Phys. Rev. Lett. **76**, 3320 (1996).
 9. F. Dias, P. Guyenne, and V. E. Zakharov, Physics Lett. **A291**, 139 (2001).
 10. V. E. Zakharov, O. A. Vasilyev, and A. I. Dyachenko, Pis'ma v ZhETF **73**, 68 (2001); (english transl. JETP Lett. **73**, 63 (2001)).
 11. V. E. Zakharov, J. Appl. Mech. Tech. Phys. **2**, 190 (1968).